J Polym Environ (2016) 24:318–327
DOI 10.1007/s10924-016-0775-6

ORIGINAL PAPER

Mechanical Properties and Isothermal Crystallization Behaviour of Poly(lactide)/Poly(methyl methacrylate)/α-Cellulose Composites

Jyh-Hong Wu[1] · Ming-Shien Yen[2] · Chien-Wen Chen[2] · M. C. Kuo[2]

Published online: 19 May 2016

Abstract Polylactide (PLA)/polymethylmethacrylate (PMMA)/α-cellulose composites were fabricated using a twin-screw extruder. During fabrication, α-cellulose short fibres were incorporated for improving the toughness of the brittle PLA and a chain extender was used for reducing PLA hydrolysis. Highly transparent PLA and PMMA were blended to obtain miscible and transparent blends. For evaluating the performance of the PLA/PMMA/α-cellulose composites, a series of measurements, including tensile and Izod impact tests, light transmission and haze measurements, thermomechanical analysis, and determination of isothermal crystallisation behaviour, was conducted. Adding the chain extender considerably reduced the occurrence of hydrolytic degradation. Both the chain extender and α-cellulose short fibres increased the elongation at break and Izod impact strength of the composites. Compared with the neat PLA, including 1.0 wt% α-cellulose short fibres increased the elongation at break and Izod impact strength of the composite PLA by approximately 211 and 219 %, respectively. According to the observed mechanical performance, the optimal blending ratios for PLA and PMMA were between 90:10 and 80:20. The total light transmittance of the composites was as high as 91 %, indicating that the PLA/PMMA blend was highly miscible. The haze value of the PLA/PMMA/α-cellulose composites was lower than 32 %. Incorporating cellulose short fibres increased the number of crystallisation sites and crystallinity of the PLA/PMMA/α-cellulose composites while reducing the spherulite dimensions.

Keywords Biomaterials · Composite materials · Polymers · Differential scanning calorimetry · Thermodynamic properties

Introduction

PLA is a biodegradable, linear aliphatic, and thermoplastic polyester and considered a promising green and biomass-derived plastic. It has attracted considerable attention because of concerns regarding CO_2 emission and environmental effects from nondegradable landfill wastes [1–5]. In recent years, many studies have examined PLA composites. Multiwalled carbon nanotubes (MWCNTs) impart electric or magnetic characteristics to PLA nanocomposites [6, 7]. Poly (L-lactide) (PLLA)/polyhedral oligomeric silsesquioxane nanocomposites were prepared through solution casting to increase the crystallisation rate and improve their mechanical properties [8].

In addition, natural fillers have been used for reinforcing PLA. Jonoobi et al. [9] used cellulose nanofibers (CNFs) for reinforcing PLA. Pei et al. used rodlike cellulose nanocrystals (CNCs) or silyate cellulose nanocrystals (SCNCs) for reinforcing PLLA by using solution casting. The authors revealed that compared with the neat PLLA, the resulting PLLA composites had an increased tensile modulus and increased tensile strength. However, the toughness improvement of the PLA/CNF, PLLA/CNC, and PLLA/SCNC nanocomposites was not estimated. [10]. Bledzki and Jaszkiewicz [11] used rayon (cellulosic

✉ M. C. Kuo
muchen@mail.ksu.edu.tw

1 Materials and Chemical Research Laboratories, Industrial Technology Research Institute, Tainan 70955, Taiwan, Republic of China

2 Department of Materials Engineering, Kun Shan University, No. 195, Kun-Da Rd., Yong-Kang District, Tainan 71070, Taiwan, Republic of China

monofilament fibre from pulp with a diameter of approximately 12 μm) and jute bundle fibres for reinforcing PLA. Rayon and jute fibres at 30 wt% increased the notch impact strength of PLA from approximately 2.4 kJ/m^2 for neat PLA to 7.5 and 3.5 kJ/m^2 for PLA/jute and PLA/rayon composites, respectively. In our previous study, natural and as-received α-cellulose short fibres were used for reinforcing brittle PLA. We demonstrated that PLA/α-cellulose composites with low α-cellulose content maintained their transparency and exhibited toughness three times higher than that of the neat PLA [5].

PMMA is a glassy and transparent polymer and can be used in the packaging industry and optical or biomedical applications [12, 13] because of its high strength, optical clarity, desirable dimensional stability, and weatherability. According to differential scanning calorimetry (DSC) scans, blending PMMA with PLLA showed a single glass transition temperature when the PLLA content was less than 20 % or more than 90 %, indicating that PLLA/PMMA blends exhibit complete miscibility when the PLLA content is less than 20 %. However, blending amorphous poly ($_D$-lactide) (PDLA) with PMMA results in a high degree of miscibility [14].

In our previous study on PLA/PMMA/SiO_2 composites, we demonstrated that nanosilica particles increased the Young's modulus and Izod impact strength of the composites. Compared with neat PLA, adding 0.5 wt% nanosilica particles increased the elongation at break and Izod impact strength by approximately 287 and 163 %, respectively. The total light transmittance of the PLA/PMMA/SiO_2 composites reached 91 %, indicating that the PLA/PMMA blend was highly miscible [15].

α-Cellulose short fibres are undissolved residues of natural pulp in an 18 % NaOH aqueous solution. Short fibres in a polymer matrix were proposed to absorb large quantities of energy through fibre pull-out [16]. Accordingly, we used α-cellulose fibres, natural cellulose short fibres, for increasing the likelihood of fibre pull-out and the microcrack lengths of the PLA matrix during fracture and for toughening the brittle PLA. However, α-cellulose is a hydrophilic natural polymer and is more polar than nanosilica particles. In the present study, a chain extender was used for improving the thermal hydrolysis and processability of PLA. Both the chain extender and α-cellulose short fibres were incorporated into PLA/PMMA blends for fabricating PLA/PMMA/α-cellulose composites. The resulting composites were designed for improving the toughness of the brittle PLA matrix, reducing the hydrolytic degradation of PLA, and maintaining the high transparency of light while sufficiently increasing the haze value of the PLA/PMMA/α-cellulose composites.

Experimental

Materials

PLA (NatureWorks 4032D) was purchased from NatureWorks Company, and it contains 92 % $_L$-lactide and 8 % meso-lactide. The molecular weight (M_w) and density of PLA are 1.8×10^5–2.0×10^5 g/mol and 1.25 g/cm^3, respectively. PMMA (Acryrex CM-205) was purchased from Chi-Mei Corporation, Taiwan. The molecular weight (M_w), density and melt index (MI) of PMMA are 3.0×10^5–3.5×10^5 g/mol, 1.19 g/cm^3, and 1.8 g/10 min (at 230 °C and 3.8 kg), respectively. Chain extender (Joncryl ADR 4368S), which is a styrene-acrylic multi-functional-epoxide oligomeric agent, was purchased from BASF, and its molecular weight and density are 6.8×10^3 g/mol and 1.08 g/cm^3, respectively. α-Cellulose short fibers measuring 200–600 μm, were purchased from Sigma, USA.

Surface Modification of α-Cellulose

As-received α-cellulose short fibres were subjected to surface modification by using stearic acid for imparting hydrophobic characteristics on the surface of the α-cellulose short fibres. The stearic acid ($M_w = 284.48$ g/mol, $mp = 68$–71 °C, $bp = 361$ °C) [17] was initially added to isopropyl alcohol, and the resulting mixture was stirred for approximately 1 h at room temperature. α-Cellulose fibres were then added to the mixture so that the carboxylic group of stearic acid physically interacted with the α-cellulose fibres, imparting hydrophobic characteristics on them [18]. In this study, 2 % stearic acid (weight of α-cellulose fibres) was used for estimating the effect of surface modification. After surface modification, the stearic-acid-modified α-cellulose fibres were dried at 60 °C for 48 h and stored in a desiccator before use.

Fabrication of PLA/PMMA/α-Cellulose Composites

PLA/PMMA/α-cellulose composites were fabricated by mixing PLA and PMMA with stearic-acid-modified α-cellulose fibres by using a twin-screw extruder (Nanking Jia-Ya SHJ-20, China). Table 1 lists the compositions of the PLA/PMMA/α-cellulose composites, which contained 1.0 wt% α-cellulose. The chain extender content was 0.5 % of the weight of PLA. PLA and PMMA pellets were dried at 80 °C for 24 h before they were kneaded for removing moisture. PLA, PMMA, the chain extender, and α-cellulose short fibres were introduced to the extruder at 200 °C to enable efficient mixing of components. After extrusion, the resulting composites were cut into pellets

Table 1 Recipes for the preparation of PLA/PMMA/α-cellulose composites

Sample	PLA	PMMA	ADR	α-cellulose
Neat PLA	100	–	–	–
PLA/ADR	99.5	–	0.5	–
PLA/α-cellulose	98.0	–	–	1.0
PLA/PMMA/α-cellulose (90/10)	88.55	10	0.45	1.0
PLA/PMMA/α-cellulose (80/20)	78.60	20	0.40	1.0
PLA/PMMA/α-cellulose (60/40)	58.70	40	0.30	1.0
PLA/PMMA/α-cellulose (40/60)	38.80	60	0.20	1.0
Neat PMMA	–	100	–	–

The chain extender from BASF (Joncryl ADR 4368S) is denoted as ADR. All of the contents are in terms of wt%

measuring 2–3 mm. Vacuum compression moulding at 200 °C was used for preparing specimens for tensile, notch impact, and dynamic mechanical property measurements.

Tensile and Impact Tests

Room temperature tensile test was conducted in accordance with the ASTM standard D638. An Instron 3369 to determine the ultimate tensile strength (*UTS*), Young's modulus (*E*), and elongation at break (ε_b). The dog-bone shaped specimens have the dimension of 120 mm × 10.32 mm × 4.24 mm (length × width × thickness). The crosshead speed was set to be 10 mm/min. The test result is typically the average of 10 specimens. Room temperature Izod impact test was conducted in accordance with the ASTM standard D256-06a. Specimen dimension is 63.5 × 12.5 × 4.0 mm (length × width × thickness), and the notch depth is 2.5 mm. A Yang-Yi QC-639E (made in Taiwan) universal digital impact tester was applied to conduct the impact test. The Izod impact test result is typically the average of 10 specimens, and the Izod impact strength is expressed as kJ/m^2.

Light Transmission and Haze Measurements

The haze and luminous transmittance were determined according to the ASTM D 1003-11. A specimen less than 0.25 mm in thickness was used to measure by a haze meter (HM-150). Total transmittance (T_t) and diffuse transmittance (T_d) were estimated, and the percent haze was calculated as follows:

$$haze = T_d/T_t \times 100\,\%. \quad (1)$$

Dynamic Mechanical Analysis

Glass transition temperature, storage modulus, and damping factor of the resulting PLA composites were measured using a dynamic mechanical analyzer (DMA, TA Q800). A tension mode testing was applied during the DMA scans, and the scanning range was from −40 to 140 °C at a heating rate of 2 °C/min and at a frequency of 1 Hz under nitrogen atmosphere.

Isothermal Crystallization Behaviour Determination

A TA differential scanning calorimeter (TA Q2000) was applied to investigate the isothermal crystallization behaviour of the neat PLA and PLA/PMMA/α-cellulose composites. The sample was heated up to 200 °C at a rate of 10 °C/min under nitrogen atmosphere. At 200 °C, this sample was held for 5 min to remove the previous thermal history, and then it was quenched to a predetermined temperature of 135 °C to undergo the isothermal crystallization process. After the isothermal crystallization process, the sample was subsequently heated to 185 °C to conduct the second-heating run and to estimate the melting temperature (T_m).

Microstructure and Fractural Surface Observations

A Zeiss Axioskop 40A petrographic microscope (POM) was used to evaluate the spherulite dimensions of neat PLA and PLA/PMMA/α-cellulose composites under isothermal crystallization. A thin piece of sample was sandwiched between two glass coverslips and placed on a digital hot-stage under nitrogen atmosphere. The hot-stage was rapidly heated to 200 °C at 20 °C/min and held for 5 min to erase the thermal history of specimens. Then, the neat PLA or PLA/PMMA/α-cellulose melt was quenched to a predetermined temperature of 135 °C and kept at this temperature to observe spherulite morphologies of the neat PLA and PLA/PMMA/α-cellulose composites. A Jeol 6700F field emission scanning electron microscope (SEM) was used to observe the fractural surfaces of the broken specimens after tensile tests.

Results and Discussion

Dispersion of α-Cellulose in the PLA/PMMA Matrix

Figure 1 shows the fracture surfaces of neat PLA and PLA/PMMA/α-cellulose (90:10) composite. α-Cellulose short fibres were homogenously distributed in the PLA/PMMA blend. The α-cellulose short fibres were pulled from the PLA/PMMA blend (arrow, Fig. 1). A socket was left on the fracture surface of the PLA/PMMA/α-cellulose (90:10) composite when the short fibres were removed.

Room Temperature Tensile and Impact Properties of the PLA/PMMA/α-Cellulose Composites

For evaluating the performance of the PLA/PMMA/α-cellulose composites, the mechanical properties, including ultimate tensile strength, Young's modulus, elongation at break, and Izod impact strength, of the neat PLA, PMMA, and PLA/PMMA/α-cellulose composites were investigated. In Table 2, the values of *UTS*, *E*, and ε_b for the neat PLA are 64.9, 2050 MPa, and 4.54 %, respectively. Blending PLA with PMMA increased the tensile strength of the PLA/PMMA/α-cellulose composites, and the *UTS* values of the resulting composites increased with increasing PMMA content because of the high *UTS* value (73.5 MPa) of neat PMMA. The *UTS* value of the PLA/α-cellulose composite is lower than that of the neat PLA by approximately 8.0 MPa, corresponding to a 12.3 % decrement. The hydrolytic degradation of PLA during kneading might be responsible for the decrement. Oever et al. [19] reported that PLA is sensitive to hydrolytic

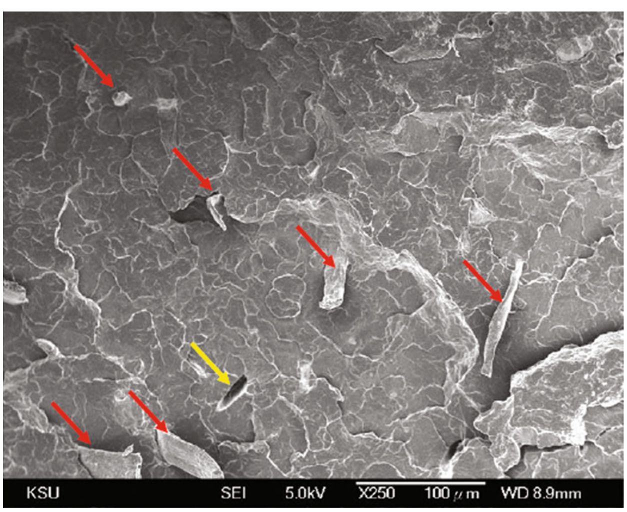

Fig. 1 The fractural surface of the tensile specimen taken from PLA/PMMA/α-cellulose (90/10) composite. The *arrow* in the micrograph shows the occurrence of fibre pull-out. A socket left when the short fibre was pulled out from the composite, as *arrow* in *yellow color* (Color figure online)

degradation under melt processing conditions. He et al. [20] proposed that incorporating multiwalled carbon nanotubes can accelerate the hydrolytic degradation of PLLA. By contrast, the *UTS* value decreased from 64.9 MPa for the neat PLA to 61.0 MPa for the PLA with a chain extender (PLA/ADR), which had no α-cellulose, corresponding to a 6.0 % decrement. Compared with the 12.3 % decrement for the PLA/α-cellulose composite, adding the chain extender during PLA melt compounding reduced the decrement of the *UTS* by approximately 51.2 % (decrement from 12.3 to 6.0 %), indicating that adding a chain extender can considerably reduce the occurrence of hydrolytic degradation.

Including α-cellulose short fibres reduced the Young's modulus of the PLA/α-cellulose composite from 2050 to 1983 MPa. In addition, adding the chain extender increased the *E* value from 2050 to 2096 MPa. Furthermore, blending PLA with PMMA considerably increased the *E* values of the composites because of the high *E* value (3300 MPa) of PMMA.

In our previous study on PLA/α-cellulose composites, including α-cellulose short fibres in the PLA polymer increased the elongation at break of the composites. A cellulose content of 4.0 wt% in the PLA matrix increased the elongation from 4.5 % for neat PLA to 6.4 % for PLA/α-cellulose composites [5]. In the present study, including a chain extender increased the elongation at break from 4.5 % for neat PLA to 10.0 % for PLA/ADR composite. As stated previously, compared with PLA/α-cellulose composites, including a chain extender in composites can reduce the occurrence of hydrolytic degradation and improve the *UTS* value. Moreover, the chain extender can improve the elongation at break of the PLA matrix. In the present study, the α-cellulose content in the PLA/PMMA blends was 1.0 wt%. Adding α-cellulose short fibres increased the elongation at break of the neat PLA from 4.5 to 8.5 % for PLA/α-cellulose composite, and this elongation at break value is lower than that of PLA/ADR. When the chain extender and α-cellulose were simultaneously added to the PLA/PMMA blend, the elongation at break of the PLA/PMMA/α-cellulose (90:10) composite reached 14.0 %. Blending PMMA with PLA reduced the ε_b value of the PLA/PMMA/α-cellulose composites because of the low ε_b value (4.6 %) of the neat PMMA. The ε_b value began decreasing from 14.0 % for the PLA/PMMA/α-cellulose (90:10) composite to 6.2 % for the PLA/PMMA/α-cellulose (40:60) composite. The optimal blending ratio was therefore between that of PLA/PMMA/α-cellulose (90:10) and that of PLA/PMMA/α-cellulose (80:20).

The aforementioned findings show that including α-cellulose can improve the elongation at break of both PLA/α-cellulose and PLA/PMMA/α-cellulose composites. Figure 2 shows the sliding behaviour that occurred in the PLA,

Table 2 The ultimate tensile strength (*UTS*), Young's modulus (*E*), elongation at break (ε_b), and Izod impact strength (*IS*) of the neat PLA, PMMA and PLA/PMMA/α-cellulose composites

Sample	*UTS* (MPa)	*E* (MPa)	ε_b (%)	*IS* (kJ/m^2)
Neat PLA	64.9 ± 2.2	2050 ± 137	4.5 ± 0.4	2.6 ± 0.3
PLA/ADR	61.0 ± 1.8	2096 ± 107	10.0 ± 1.8	5.2 ± 0.4
PLA/α-cellulose	56.9 ± 1.6	1983 ± 114	8.5 ± 1.5	6.8 ± 0.4
PLA/PMMA/α-cellulose (90/10)	60.5 ± 1.6	2186 ± 143	14.0 ± 1.9	8.3 ± 0.3
PLA/PMMA/α-cellulose (80/20)	61.9 ± 2.0	2281 ± 126	10.9 ± 2.1	7.6 ± 0.4
PLA/PMMA/α-cellulose (60/40)	62.8 ± 1.9	2509 ± 165	7.4 ± 2.0	5.3 ± 0.3
PLA/PMMA/α-cellulose (40/60)	65.0 ± 2.0	2832 ± 150	6.2 ± 1.8	4.5 ± 0.3
Neat PMMA[a]	73.5	3300	4.6	2.0

[a] The tensile properties and Izod impact strength (*IS*) of PMMA were cited from the specification of PMMA (Acryrex CM-205), Chi-Mei Corporation, Taiwan

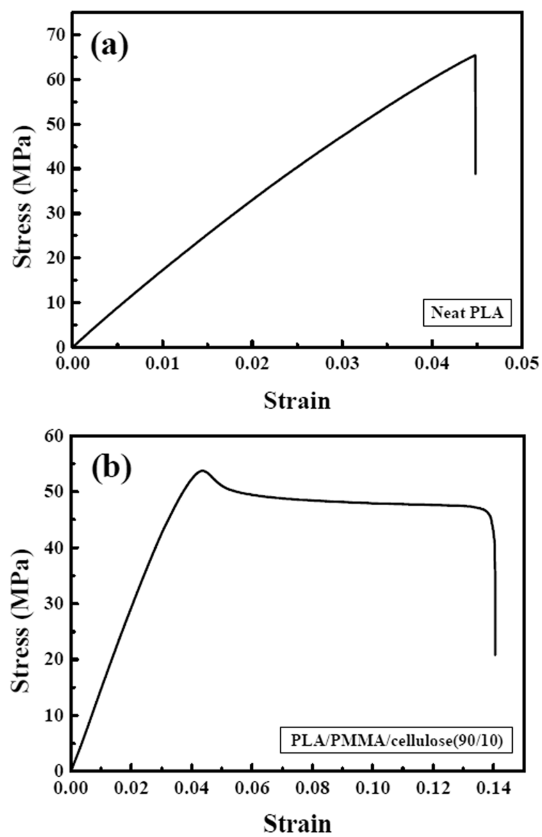

Fig. 2 The sliding behaviour induced by the inclusion of α-cellulose short fibres in the PLA/PMMA/α-cellulose composite during tensile testing. **a** Neat PLA and **b** PLA/PMMA/α-cellulose (90/10) composite

PMMA, α-cellulose composites during tensile testing. The neat PLA (Fig. 2a) was brittle; however, the PLA/PMMA/α-cellulose (90:10) composite (Fig. 2b) exhibited plastic flow and ductile behaviour. Thus, because of lubrication sliding and the ductile behaviour, including α-cellulose short fibres in PLA/PMMA blends appreciably improved the toughness of the PLA/PMMA/α-cellulose composites.

Both the chain extender and α-cellulose increased the elongation at break (Table 2) and, consequently, the Izod impact strength of the PLA/PMMA/α-cellulose composites. The *IS* value for the PLA/PMMA/α-cellulose (90:10) composite reached 8.3 kJ/m^2, representing an increment of 219 % compared with that of the neat PLA. In this study, surface-modified α-cellulose short fibres 200–600 μm in length were used. These α-cellulose short fibres dispersed homogeneously in the PLA matrix (Fig. 1), resulting in fibre pull-out [16] and improving both the elongation at break and toughness of the PLA/PMMA/α-cellulose composites.

Increasing the PMMA content in the PLA/MMA/α-cellulose composites reduces their *IS* value because of the brittleness of the PMMA polymer. The *IS* value (4.5 kJ/m^2) for a mixing ratio of 40:60 (PLA:PMMA) is higher than that (2.6 kJ/m^2) of the neat PLA, indicating that incorporating the chain extender and α-cellulose short fibres positively affected the toughness improvement of the brittle PLA/PMMA blends. Physically, adding PMMA increases the values of the ultimate tensile strength and Young's modulus of the composites but reduces their elongation at break and impact strength. However, adding the chain extender and α-cellulose fibres compensates the reduction in the ε_b and *IS* values of the PLA/PMMA/α-cellulose composites. Moreover, adding the chain extender reduces the occurrence of hydrolytic degradation and adding α-cellulose fibres imparts lubrication sliding and ductile behaviours to the composites.

Light Transmission Properties of the PLA/PMMA/α-Cellulose Composites

Table 3 shows the total light transmittance (T_t) and haze values of neat PLA, PMMA, and PLA/PMMA/α-cellulose composite films. The total light transmittance values for the neat PLA and PMMA films were 92.84 % and 93.35 %, respectively, indicating the high transparency of the PLA polymer. Moreover, a low α-cellulose content (approximately 4 wt%) in the PLA/α-cellulose composites maintained their transparency and improved their toughness by

Table 3 The total light transmittance (T_t), diffuse transmittance (T_d), and haze values of the neat PLA, PMMA, and PLA/PMMA/α-cellulose composite films

Sample	T_t (%)	T_d (%)	*Haze* (%)
Neat PLA	92.84	15.83	17.05
PLA/ADR	92.65	18.16	19.60
PLA/α-cellulose	91.62	20.42	22.29
PLA/PMMA/α-cellulose (90/10)	92.05	23.40	25.42
PLA/PMMA/α-cellulose (80/20)	92.66	25.40	27.41
PLA/PMMA/α-cellulose (60/40)	93.09	29.65	31.85
PLA/PMMA/α-cellulose (40/60)	93.20	26.43	28.36
Neat PMMA	93.35	14.76	15.81

three times that of the neat PLA [5]. Accordingly, the mixture ratio of the PLA/PMMA blends barely influenced the total light transmittance of the PLA/PMMA/α-cellulose composite films. As shown in Table 3, the T_t value increased slightly with an increasing PMMA ratio. Adding the chain extender and α-cellulose short fibres to the PLA or PLA/PMMA blends barely influenced the total light transmittance. By contrast, adding α-cellulose short fibres significantly increased the diffuse transmittance (T_d) as well as the haze value of the PLA/PMMA/α-cellulose composites. The haze value of the PLA composites increased with an increasing blending ratio of PLA in the PLA/PMMA blends, increasing from 22.29 for PLA/α-cellulose to 31.85 for PLA/PMMA/α-cellulose (60:40) composite and then decreasing to 28.36 for PLA/PMMA/α-cellulose (40:60) composite. The increase in the haze value of the PLA/PMMA/α-cellulose composites might be attributable to microphase separation in the PLA/PMMA blends. Eguiburu et al. proposed that segregated crystalline microdomains existed in PLLA/PMMA blends [13].

The boundaries among the PLLA crystallites may diffuse the paths of visible light. Because of the addition of α-cellulose short fibres and the microdomains of crystalline PLA, the haze value of the PLA/PMMA/α-cellulose composites considerably increased compared with that of the neat PLA and PMMA. The increase in the haze value of the PLA/PMMA/α-cellulose composites is not completely a drawback. Instead, adequately increasing the haze value but maintaining the same total light transmittance might enhance the performance of the PLA/PMMA/α-cellulose composites in LED lighting masks.

Thermomechanical Properties of the PLA/PMMA/α-Cellulose Composites

As shown in Fig. 3a, adding a chain extender increased the storage modulus of the PLA polymer, but adding cellulose

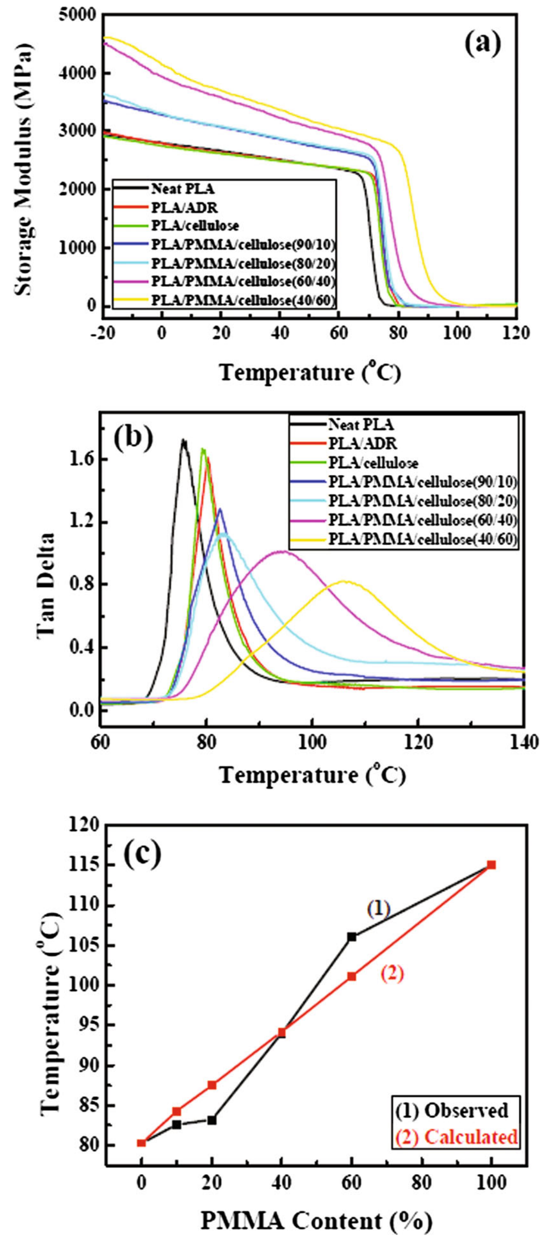

Fig. 3 The spectra of **a** storage modulus and **b** Tan delta of the neat PLA, PLA/α-cellulose, and PLA/PMMA/α-cellulose composites. Plot **c** is the observed and calculated glass transition temperatures of the PLA/PMMA/α-cellulose composites

fibres slightly decreased that of the PLA/α-cellulose composite. Blending PLA with stiff PMMA increased the storage modulus of the PLA/PMMA/α-cellulose composites, and the value increased with increasing PMMA content. As stated previously, a chain extender increased the *E* value from 2050 to 2186 MPa for neat PLA and PLA/ADR, respectively. However, incorporating cellulose fibres slightly reduced the *E* value from 2050 MPa for the neat PLA to 1983 MPa for the PLA/α-cellulose composite because of hydrolytic degradation. Blending PLA with stiff PMMA increased the E values of the PLA/PMMA/α-cellulose composite (Table 2). The storage spectra of the neat PLA and PLA/ADR and PLA/PMMA/α-cellulose composites are consistent with the bulk modulus (Young's modulus) of these composites.

As shown in Fig. 3b, the *Tan* δ spectrum of each PLA/PMMA/α-cellulose composite exhibited a single peak, suggesting no microphase separation in the PLA/PMMA blends. The peak values of the *Tan* δ spectra of PLA/ADR, PLA/α-cellulose, and PLA/PMMA/SiO_2 composites are lower than that of neat PLA. The peak value decreases with increasing PMMA content, indicating that introducing a chain extender, α-cellulose, or brittle PMMA substantially reduces the damping property of neat PLA. As shown in Table 2, including a chain extender and cellulose short fibres increased the values of elongation at break and Izod impact strength of the PLA/ADR and PLA/α-cellulose composite. The events in tensile and impact tests seem to reverse the decreases in the damping factors of the PLA/ADR, PLA/α-cellulose, and PLA/PMMA/α-cellulose composites. As stated previously, major sliding in the PLA/PMMA/α-cellulose composites occurs in the plastic region but not in the elastic region (Fig. 2). However, during dynamic mechanical analysis measurement, the magnitude of the applied sinusoidal deformation is linear and too minuscule to cause apparent sliding in the PLA matrix, unlike the massive fractural forces in tensile and impact tests. Therefore, the decrease in the damping factor of the PLA/PMMA/α-cellulose composites might be associated with the increase in their E values instead of the decreases in their ε_b and IS values.

The glass transition temperature (T_g) of the PLA/PMMA/α-cellulose composites can be estimated according to their Tan δ peak. Moreover, the calculated T_g value can be estimated using the following equation [21]:

$$\frac{1}{T_g} = \frac{w_1}{T_g^1} + \frac{w_2}{T_g^2}, \tag{2}$$

where T_g^1, T_g^2, and T_g are the glass transition temperatures (in K) of the PLA/α-cellulose composites, neat PMMA, and PLA/PMMA/α-cellulose composites, respectively. The values of T_g^1 and T_g^2 are 253.45 K (80.3 °C) and 388.15 K (115 °C), respectively [22]. Furthermore, w_1 and w_2 are the weight fractions of PLA and PMMA, respectively. Figure 3c shows the observed and calculated glass transition temperatures of the PLA/PMMA/α-cellulose composites. The T_g value of the composites increases as the PMMA weight fraction increases because of the high T_g value (115 °C) of the neat PMMA. Blending PLA with PMMA significantly increases the glass transition temperature of the PLA/PMMA/α-cellulose composites.

Isothermal Crystallization Behavior of PLA/PMMA/α-Cellulose Composites

The isothermal crystallisation of the neat PLA and PLA/ADR, PLA/α-cellulose, and PLA/PMMA/α-cellulose composites was conducted using DSC at a predetermined temperature of 135 °C for 120 min (Fig. 4). The crystallisation enthalpies (ΔH_c) and peak crystallisation times (τ_p) of the neat PLA and its composites were determined. The absolute crystallinities (X_c) of the neat PLA and its composites were estimated using the heat of fusion of an infinitely thick PLA crystal, ΔH_f^o, as follows [23, 24]:

$$X_c = \frac{\Delta H_c}{\Delta H_f^o W_{polymer}} \times 100, \tag{3}$$

where ΔH_f^o is approximately 93.7 J/g [25] and $W_{polymer}$ is the weight fraction of the polymer matrix. The melting temperature was estimated from the second heating run (Fig. 5). These crystallisation parameters are shown in Table 4.

As shown in Table 4, the crystallinity of the neat PLA isothermally crystallised at 135 °C was 46.8 %. Incorporating a chain extender reduced the X_c value to 40.6 %, but incorporating α-cellulose short fibres increased this value to 48.4 %. This increase in the crystallinity of the PLA/α-cellulose composite may be attributed to the additional deposition sites available when the α-cellulose short fibres are incorporated. Incorporating a chain extender improved hydrolysis through reactions between the epoxy group of the chain extender and the carboxyl and hydroxyl end groups of the PLA polymer. However, the chain extender might produce long-chain branched structures [26] and reduce the crystallinity of the PLA/ADR compared with that of the neat PLA. Moreover, blending PLA with amorphous PMMA hindered the diffusion of crystalline

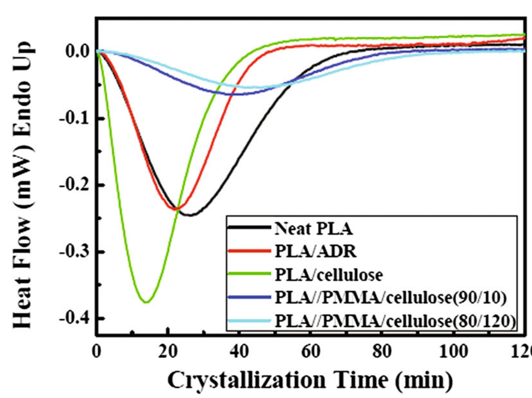

Fig. 4 The DSC crystallisation traces for the neat PLA, PLA/α-cellulose, and PLA/PMMA/α-cellulose composites isothermally crystallised at 135 °C

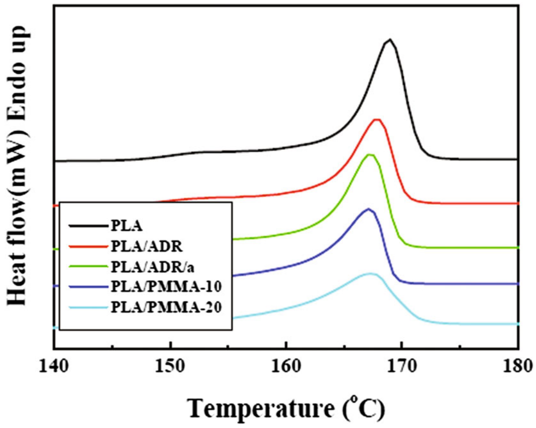

Fig. 5 The second DSC heating traces for the neat PLA, PLA/α-cellulose, and PLA/PMMA/α-cellulose composites isothermally crystallised at 135 °C

Table 4 The melting temperatures (T_m), absolute crystallinities (X_c), and peak crystallisation times (τ_p) of the neat PLA, PLA/ADR, PLA/α-cellulose, and PLA/PMMA/α-cellulose composites isothermally crystallised at 135 °C

Sample	T_m (°C)	X_c (%)	τ_p (min)
Neat PLA	168.9	46.8	25.9
PLA/ADR	167.8	40.6	22.1
PLA/α-cellulose	167.3	48.4	13.9
PLA/PMMA/α-cellulose (90/10)	167.2	37.3	39.6
PLA/PMMA/α-cellulose (80/20)	167.2	34.7	44.9

PLA molecules and considerably reduced the crystallinity of the PLA/PMMA/α-cellulose composites. The Xc value for PLA/α-cellulose was 48.4 %, whereas those for PLA/PMMA/α-cellulose (90:10) and PLA/PMMA/α-cellulose (80:20) were as low as 37.3 and 34.7 %, respectively. No exothermic or melting peak was observed when the PLA content in the PLA/PMMA/α-cellulose composites was less than 20 %. Eguiburu et al. [14] suggested that observing the crystallisation and melting of PLLA crystals is possible during the second run when the PLLA content in the PLLA/PMMA blend is more than 80 %. Our observation of the crystallisation behaviour of the PLA/PMMA/α-cellulose composites is consistent with that of Eguiburu et al.

The peak crystallisation time (τ_p) was used for defining the time from onset to a point where the exothermic peak appeared under isothermal crystallisation. As previously reported, the peak crystallisation time is equal to the crystallisation half-life when the DSC crystallisation trace is symmetric [27, 28]. As shown in Fig. 4 and Table 4, incorporating α-cellulose significantly reduced the τ_p value from 25.9 min for the neat PLA to 13.9 min for the PLA/α-cellulose composite. Including α-cellulose in the PLA matrix increased the crystallinity of the PLA/α-cellulose composite but reduced the peak crystallisation time. One explanation for these changes is that the α-cellulose short fibres increase the number of deposition sites but reduce the molecular mobility of PLA chain segments. Consequently, the PLA chain segments diffuse over a shorter distance before being deposited on a nucleus. Incorporating a chain extender also reduced the peak crystallisation time of the composites compared with that of the neat PLA. However, blending PLA with amorphous PMMA considerably hindered the diffusion of crystalline PLA molecules and increased the τ_p value of the PLA/PMMA/α-cellulose composites.

The spherulite morphology of PLA could account for the above pictures. The dimensions of the PLA spherulites decreased continuously from approximately 46 µm for the neat PLA to 19 µm for the PLA/PMMA/α-cellulose (80:20) composite (Fig. 6). Including α-cellulose fibres increased the number of crystallisation sites but reduced the dimensions of spherulites of the PLA/α-cellulose composites during crystallisation. However, blending crystalline PLA with amorphous PMMA reduced the number of crystallisation sites and increased hindrance of crystalline PLA molecule diffusion because of the higher glass-transition temperature of the PLA/PMMA/α-cellulose composites (Fig. 3c). Increasing the number of crystallisation sites or the hindrance of PLA molecule diffusion during crystallisation reduces the spherulite dimensions and causes more defects in the PLA crystallites. Regarding the melting temperatures of the neat PLA and PLA/α-cellulose composite, incorporating a chain extender slightly decreased the T_m value (Table 4). The α-cellulose fibres increased both the number of crystallisation sites and crystallinity, but simultaneously reduced the spherulite dimensions of the PLA/α-cellulose composites. Introducing α-cellulose fibres creates smaller spherulites exhibiting more defects than larger spherulites do and reduces the melting temperature of the PLA/α-cellulose composites. Furthermore, because this process occurs in the PLA/α-cellulose composite, blending amorphous PMMA into PLA introduces more defects into the crystalline PLA matrix and further reduces the melting temperature (Table 4).

Correlations Between Physical and Crystallization Properties

The crystallisation behaviour of the PLA/PMMA/α-cellulose composites may reflect the mechanical properties of PLA composites. In this study, both a chain extender and PMMA increased the E values of the PLA/ADR and PLA/PMMA/α-cellulose composites. Moreover, compared with

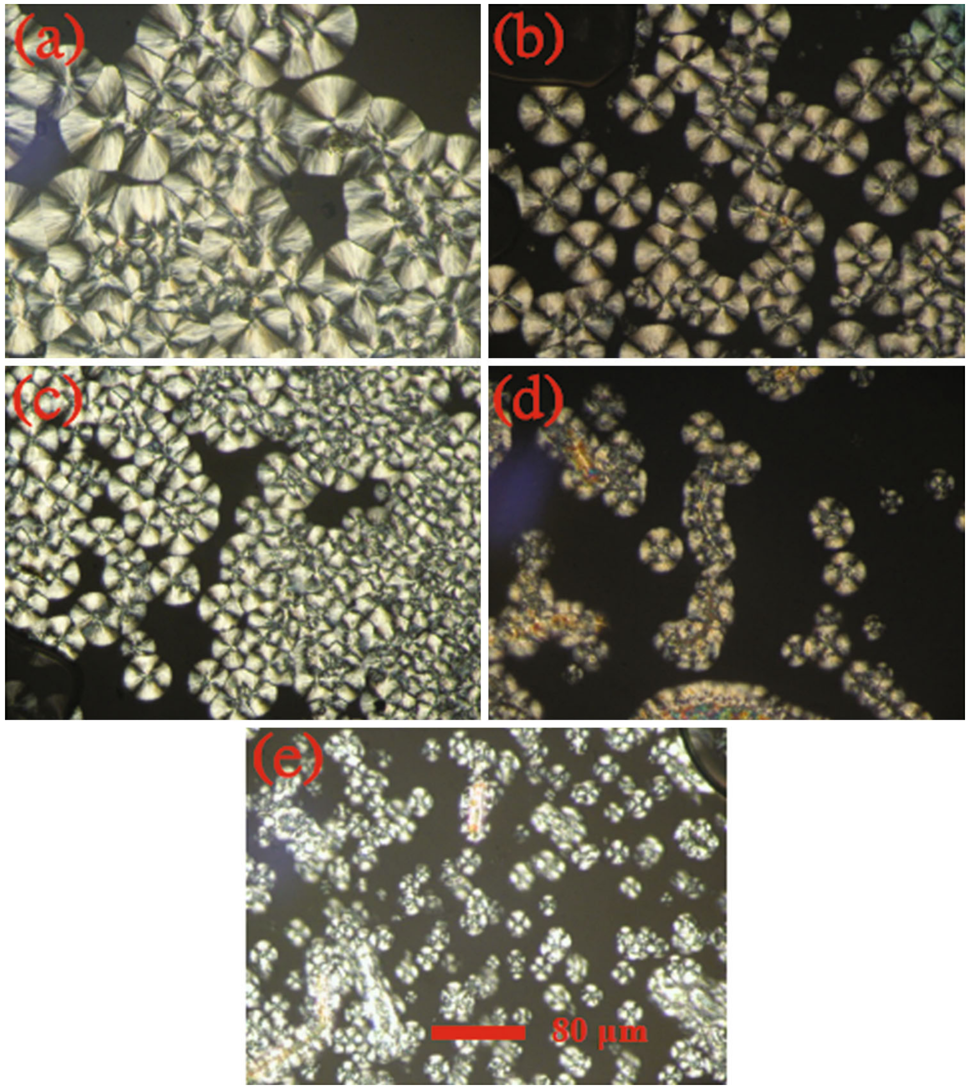

Fig. 6 The spherulite dimensions of neat PLA, PLA/ADR, PLA/α-cellulose, and PLA/PMMA/α-cellulose composites isothermally crystallised at 135 °C for 10 min. The spherulite dimensions for **a** neat PLA, **b** PLA/ADR, **c** PLA/α-cellulose, **d** PLA/PMMA/α-cellulose (90/10), **e** PLA/PMMA/α-cellulose (80/20) composites are approximately 46, 32, 26, 23, and 19 μm, respectively

the neat PLA, including a chain extender and α-cellulose fibres improved the ε_b and notch *IS* values of the PLA/PMMA/α-cellulose composites. The decrease in the spherulite dimensions (Fig. 6) may account for the improved ε_b and notch *IS* values of the PLA/PMMA/α-cellulose composites. The smaller crystallites in the PLA/PMMA/α-cellulose composites may easily induce grain boundary sliding, increasing the εb and improving the *IS* values of the PLA/PMMA/α-cellulose composites. Furthermore, the formation of smaller spherulites may increase the boundary grain region (spherulites) with higher limits of elasticity and plasticity and increase the amorphous phase facing the crystalline zone. Consequently, incorporating the chain extender and α-cellulose into the PLA/PMMA blends increases the number of crystallisation sites and imparts smaller crystallites to the PLA polymer, thus improving the *E*, ε_b, and *IS* values of the PLA composites.

The crystallisation behaviour might also influence the light transmission properties of the PLA/PMMA/α-cellulose composites. Lin et al. used atomic force microscopy for characterising the roughness of biaxially oriented polypropylene film surfaces. The authors proposed that the large-scale rough surface is created primarily by the spherulites, which may be as large as 200 μm in polypropylene films, and spherulite boundaries. Surface roughness on the submicron scale, possibly resulting from the lamellar or fibrillar structure, did not affect transparency [29]. In the present study, the spherulite dimensions for the PLA/PMMA/α-cellulose composites were approximately 19–46 μm, which is considerably lower than 200 μm. Including α-cellulose increased the crystallinity from 46.8 % for the neat PLA to 48.4 % for the PLA/α-cellulose composites. This inclusion barely influenced the total light transmittance of the composites. The decreases in spherulite dimensions in the PLA composites might compensate for the opposite effects of increased spherulite boundaries on the total light transmittance. However, adding α-cellulose and the microdomains of crystalline PLA may diffuse the paths of visible light and increase the haze value of the PLA/PMMA/α-cellulose composites compared with those of the neat PLA and PMMA.

Conclusions

In this study, a chain extender, α-cellulose short fibres, and PMMA were incorporated into the brittle and transparent PLA polymer. Both the chain extender and α-cellulose short fibres increased the elongation at break and Izod impact strength of the PLA/PMMA/α-cellulose composites. Compared with the neat PLA, including 1.0 wt% cellulose short fibres increased the elongation at break and Izod impact strength of the composites by approximately 211 and 219 %, respectively. Blending PLA with PMMA increased the *UTS* and *E* values of the PLA/PMMA/α-cellulose composites, but reduced the ε_b and *IS* values. Accordingly, optimal blending ratios for PLA, PMMA, and α-cellulose were between 90:10 and 80:20. Furthermore, PLA/PMMA blends maintained a high degree of transparency. Including cellulose fibres in the PLA/PMMA blends increased the haze value of the PLA/PMMA/α-cellulose composites and maintained the high total light transmittance. All haze values of the PLA/PMMA/α-cellulose composites were lower than 32 %. This adequate haze value could lower the LED characteristic of point-light sources and evenly distribute the LED light from polymer lamp masks. Accordingly, PLA/PMMA/α-cellulose composites have high potential for application in the field of LED lamp masks.

Acknowledgments The authors gratefully acknowledge the sponsorship from Ministry of Science and Technology, Taiwan, ROC, under the Project No. NSC 103-2221-E-168-035.

References

1. Lai WH, Liao JP (2013) Mater Chem Phys 139:161
2. Bitinis N, Verdejo R, Cassagnau P, Lopez-Manchado MA (2011) Mater Chem Phys 129:823
3. Hu Y, Rogunova M, Topolkaraev V, Hiltner A, Baer E (2003) Polymer 44:5701
4. Anderson KS, Hillmyer MA (2004) Polymer 45:8809
5. Wu JH, Kuo MC, Chen CW, Hsu YL, Kuan PH, Lee KY, Fang KT, He JH (2013) Polym Plast Technol Eng 52:877
6. Villmow T, Potschke P, Pegel S, Haussler L, Kretzschmar B (2008) Polymer 49:3500
7. Feng J, Cai W, Sui J, Li Z, Wan J, Chakoli AN (2008) Polymer 49:4989
8. Qiu Z, Pan H (2010) Compos Sci Technol 70:1089
9. Jonoobi M, Harun J, Mathew AP, Oksman K (2010) Compos Sci Technol 70:1742
10. Pei A, Zhou Q, Berglund LA (2010) Compos Sci Technol 70:815
11. Bledzki A, Jaszkiewicz KA (2010) Compos Sci Technol 70:1687
12. Vega-González A, Subra-Paternault P, López-Periago AM, García-González CA, Domingo C (2008) Eur Polymer J 44:1081
13. Fischer B, Ziadeh M, Pfaff A, Breuosef J, Altstädt V (2012) Polymer 53:3230
14. Eguiburu JL, Iruin JJ, Fernandez-Berridi MJ, San Román J (1998) Polymer 39:6891
15. Wu JH, Kuo MC, Chen CW (2015) J Appl Polym Sci 132:42378
16. Hul D (1981) An introduction to composite materials. Cambridge University Press, Cambridge, p 81
17. Ahn SH, Kim SH, Lee SG (2004) J Appl Polym Sci 94:812
18. Lin Y, Chen H, Chan CM, Wu J (2008) Macromolcules 41:9204
19. van den Oever MJA, Beck B (2010) J Mussig Compos A 41:1628
20. He L, Sun J, Wang X, Fan X, Zhao Q, Cai L, Song R, Ma Z, Huang W (2012) Mater Chem Phys 134:1056
21. Lee JC, Litt Morton H (2000) Polym J 32:228
22. Ray SS, Yamada K, Okamoto M, Ueda K (2003) Polymer 44:857
23. Wu JH, Yen MS, Kuo MC, Chen BH (2013) Mater Chem Phys 142:726
24. Arrighi V, McEwen IJ, Qian H, Serrano Prieto MB (2003) Polymer 44:6259
25. Hilker B, Fields KB, Stern A, Space B, Zhang XP, Harmon JP (2010) Polymer 51:4790
26. Antoine LD, Peter D, Christophe B (2010) Compos Sci Technol 70:231
27. Najafi N, Heuzey MC, Carreau PJ, Wood-Adams PM (2012) Polym Degrad Stab 97:554
28. Munehisa Y, Shinsuke T, Koji I, Yoshinori O, Yusuke D, Kazuhisa T (2006) Polymer 47:7554
29. Lin YJ, Dias P, Chum S, Hiltner A, Baer E (2007) Soc Plast Eng 47:1658